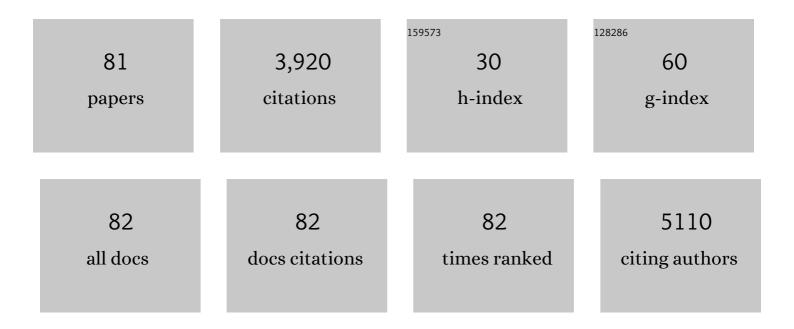
Matthew E Merritt

List of Publications by Year in descending order

Source: https://exaly.com/author-pdf/9392208/publications.pdf Version: 2024-02-01



#	Article	IF	CITATIONS
1	Application of Counter-Wound Multi-Arm Spirals in HTS Resonator Design. IEEE Transactions on Applied Superconductivity, 2022, 32, 1-4.	1.7	1
2	INCA 2.0: A tool for integrated, dynamic modeling of NMR- and MS-based isotopomer measurements and rigorous metabolic flux analysis. Metabolic Engineering, 2022, 69, 275-285.	7.0	32
3	Detecting de novo Hepatic Ketogenesis Using Hyperpolarized [2-13C] Pyruvate. Frontiers in Physiology, 2022, 13, 832403.	2.8	3
4	Ex Vivo Hepatic Perfusion Through the Portal Vein in Mouse. Journal of Visualized Experiments, 2022, , .	0.3	1
5	Editorial for " <scp>Wholeâ€Abdomen</scp> Metabolic Imaging of Healthy Volunteers Using Hyperpolarized [<scp>1â€¹³C</scp>]pyruvate <scp>MRlâ€</scp> . Journal of Magnetic Resonance Imaging, 2022, 56, 1807-1808.	3.4	0
6	Lipogenesis mediated by OGR1 regulates metabolic adaptation to acid stress in cancer cells via autophagy. Cell Reports, 2022, 39, 110796.	6.4	13
7	Real Time Measurement of Hepatic βâ€oxidation with Deuterium Magnetic Resonance in Murine Models on a High Fat Diet. FASEB Journal, 2022, 36, .	O.5	0
8	¹⁵ Nâ€carnitine, a novel endogenous hyperpolarized MRI probe with long signal lifetime. Magnetic Resonance in Medicine, 2021, 85, 1814-1820.	3.0	11
9	Application of Carbon-13 Isotopomer Analysis to Assess Perinatal Myocardial Glucose Metabolism in Sheep. Metabolites, 2021, 11, 33.	2.9	2
10	Deuterated water imaging of the rat brain following metabolism of [² H ₇]glucose. Magnetic Resonance in Medicine, 2021, 85, 3049-3059.	3.0	16
11	Insulin resistance is mechanistically linked to hepatic mitochondrial remodeling in non-alcoholic fatty liver disease. Molecular Metabolism, 2021, 45, 101154.	6.5	33
12	Comparison of selective excitation and multi-echo chemical shift encoding for imaging of hyperpolarized [1-13C]pyruvate. Journal of Magnetic Resonance, 2021, 325, 106927.	2.1	4
13	Targeted and Untargeted Liver Metabolomics Demonstrate Key Differences of Perchloric acid and Acetonitrile Isopropanol Water Extraction Through Gas Chromatography Mass Spectrometry. FASEB Journal, 2021, 35, .	0.5	0
14	Intraspecific variation in polar and nonpolar metabolite profiles of a threatened Caribbean coral. Metabolomics, 2021, 17, 60.	3.0	5
15	Hyperpolarized Dihydroxyacetone Is a Sensitive Probe of Hepatic Gluconeogenic State. Metabolites, 2021, 11, 441.	2.9	7
16	Measuring NQO1 Bioactivation Using [2H7]Glucose. Cancers, 2021, 13, 4165.	3.7	8
17	ROS and hypoxia signaling regulate periodic metabolic arousal during insect dormancy to coordinate glucose, amino acid, and lipid metabolism. Proceedings of the National Academy of Sciences of the United States of America, 2021, 118, .	7.1	28
18	Branched chain amino acids and carbohydrate restriction exacerbate ketogenesis and hepatic mitochondrial oxidative dysfunction during NAFLD. FASEB Journal, 2020, 34, 14832-14849.	0.5	19

#	Article	IF	CITATIONS
19	HDO production from [2H7]glucose Quantitatively Identifies Warburg Metabolism. Scientific Reports, 2020, 10, 8885.	3.3	18
20	A noninvasive method to study the evolution of extracellular fluid volume in mice using time-domain nuclear magnetic resonance. American Journal of Physiology - Renal Physiology, 2020, 319, F115-F124.	2.7	8
21	Aqueous humor metabolite profile of pseudoexfoliation glaucoma is distinctive. Molecular Omics, 2020, 16, 425-435.	2.8	28
22	The influence of Ho3+ doping on 13C DNP in the presence of BDPA. Physical Chemistry Chemical Physics, 2019, 21, 18629-18635.	2.8	2
23	Single-walled carbon nanotubes repress viral-induced defense pathways through oxidative stress. Nanotoxicology, 2019, 13, 1176-1196.	3.0	13
24	Remodeling of substrate consumption in the murine sTAC model of heart failure. Journal of Molecular and Cellular Cardiology, 2019, 134, 144-153.	1.9	16
25	Loss of EZH2 Reprograms BCAA Metabolism to Drive Leukemic Transformation. Cancer Discovery, 2019, 9, 1228-1247.	9.4	107
26	Regulation of renal NaDC1 expression and citrate excretion by NBCe1-A. American Journal of Physiology - Renal Physiology, 2019, 317, F489-F501.	2.7	13
27	Metabolomic profiles differ among unique genotypes of a threatened Caribbean coral. Scientific Reports, 2019, 9, 6067.	3.3	38
28	Cancer in the crosshairs: targeting cancer metabolism with hyperpolarized carbonâ€13 MRI technology. NMR in Biomedicine, 2019, 32, e3937.	2.8	10
29	Hyperpolarized 13C MRI: Path to Clinical Translation in Oncology. Neoplasia, 2019, 21, 1-16.	5.3	316
30	Kinetic Analysis of Hepatic Metabolism Using Hyperpolarized Dihydroxyacetone. Journal of Chemical Information and Modeling, 2019, 59, 605-614.	5.4	6
31	Nuclear Magnetic Resonance Measurement of Metabolic Flux Using 13C and 1H Signals. Methods in Molecular Biology, 2019, 1996, 29-40.	0.9	4
32	Probing cardiac metabolism by hyperpolarized 13 <scp>C MR</scp> using an exclusively endogenous substrate mixture and photoâ€induced nonpersistent radicals. Magnetic Resonance in Medicine, 2018, 79, 2451-2459.	3.0	18
33	In vivo hyperpolarization transfer in a clinical MRI scanner. Magnetic Resonance in Medicine, 2018, 80, 480-487.	3.0	7
34	The effect of Ho ³⁺ doping on ¹³ C dynamic nuclear polarization at 5 T. Physical Chemistry Chemical Physics, 2018, 20, 728-731.	2.8	4
35	Sensitivity enhancement for detection of hyperpolarized ¹³ C MRI probes with ¹ H spin coupling introduced by enzymatic transformation in vivo. Magnetic Resonance in Medicine, 2018, 80, 36-41.	3.0	9
36	A novel inhibitor of pyruvate dehydrogenase kinase stimulates myocardial carbohydrate oxidation in diet-induced obesity. Journal of Biological Chemistry, 2018, 293, 9604-9613.	3.4	24

#	Article	IF	CITATIONS
37	Multiband spectral-spatial RF excitation for hyperpolarized [2- ¹³ C]dihydroxyacetone ¹³ C-MR metabolism studies. Magnetic Resonance in Medicine, 2017, 77, 1419-1428.	3.0	14
38	Hyperpolarized δâ€{1â€ ¹³ C]gluconolactone as a probe of the pentose phosphate pathway. NMR in Biomedicine, 2017, 30, e3713.	2.8	21
39	A comprehensive analysis of myocardial substrate preference emphasizes the need for a synchronized fluxomic/metabolomic research design. American Journal of Physiology - Heart and Circulatory Physiology, 2017, 312, H1215-H1223.	3.2	9
40	Using a novel NQO1 bioactivatable drug, betaâ€lapachone (ARQ761), to enhance chemotherapeutic effects by metabolic modulation in pancreatic cancer. Journal of Surgical Oncology, 2017, 116, 83-88.	1.7	24
41	The NQO1 bioactivatable drug, β-lapachone, alters the redox state of NQO1+ pancreatic cancer cells, causing perturbation in central carbon metabolism. Journal of Biological Chemistry, 2017, 292, 18203-18216.	3.4	72
42	Monitoring acute metabolic changes in the liver and kidneys induced by fructose and glucose using hyperpolarized [2â€ ¹³ C]dihydroxyacetone. Magnetic Resonance in Medicine, 2017, 77, 65-73.	3.0	28
43	A general chemical shift decomposition method for hyperpolarized ¹³ C metabolite magnetic resonance imaging. Magnetic Resonance in Chemistry, 2016, 54, 665-673.	1.9	7
44	Measuring changes in substrate utilization in the myocardium in response to fasting using hyperpolarized [1-13C]butyrate and [1-13C]pyruvate. Scientific Reports, 2016, 6, 25573.	3.3	34
45	Metabolism of hyperpolarized [1â€ ¹³ C]pyruvate through alternate pathways in rat liver. NMR in Biomedicine, 2016, 29, 466-474.	2.8	41
46	Accelerated chemical shift imaging of hyperpolarized ¹³ C metabolites. Magnetic Resonance in Medicine, 2016, 76, 1033-1038.	3.0	14
47	Use of a Multi-compartment Dynamic Single Enzyme Phantom for Studies of Hyperpolarized Magnetic Resonance Agents. Journal of Visualized Experiments, 2016, , e53607.	0.3	3
48	Hyperpolarized ¹³ C NMR detects rapid drugâ€induced changes in cardiac metabolism. Magnetic Resonance in Medicine, 2015, 74, 312-319.	3.0	35
49	Hyperpolarized 13C Magnetic Resonance and Its Use in Metabolic Assessment of Cultured Cells and Perfused Organs. Methods in Enzymology, 2015, 561, 73-106.	1.0	30
50	Production of hyperpolarized 13CO2 from [1-13C]pyruvate in perfused liver does reflect total anaplerosis but is not a reliable biomarker of glucose production. Metabolomics, 2015, 11, 1144-1156.	3.0	20
51	Kinetic Modeling and Constrained Reconstruction of Hyperpolarized [1-13C]-Pyruvate Offers Improved Metabolic Imaging of Tumors. Cancer Research, 2015, 75, 4708-4717.	0.9	69
52	Mitochondrial metabolism mediates oxidative stress and inflammation in fatty liver. Journal of Clinical Investigation, 2015, 125, 4447-4462.	8.2	320
53	Real-time Detection of Hepatic Gluconeogenic and Glycogenolytic States Using Hyperpolarized [2-13C]Dihydroxyacetone. Journal of Biological Chemistry, 2014, 289, 35859-35867.	3.4	55
54	Propionate stimulates pyruvate oxidation in the presence of acetate. American Journal of Physiology - Heart and Circulatory Physiology, 2014, 307, H1134-H1141.	3.2	19

#	Article	IF	CITATIONS
55	Hyperpolarized Magnetic Resonance as a Sensitive Detector of Metabolic Function. Biochemistry, 2014, 53, 7333-7357.	2.5	143
56	Glutamine Oxidation Maintains the TCA Cycle and Cell Survival during Impaired Mitochondrial Pyruvate Transport. Molecular Cell, 2014, 56, 414-424.	9.7	504
57	Metabolic characteristics of human hearts preserved for 12 hours by static storage, antegrade perfusion, or retrograde coronary sinus perfusion. Journal of Thoracic and Cardiovascular Surgery, 2014, 148, 2310-2315.e1.	0.8	13
58	Influence of deuteration in the glassing matrix on 13C dynamic nuclear polarization. Physical Chemistry Chemical Physics, 2013, 15, 7032.	2.8	46
59	Electron spin resonance studies of trityl OX063 at a concentration optimal for DNP. Physical Chemistry Chemical Physics, 2013, 15, 9800.	2.8	81
60	The efficiency of DPPH as a polarising agent for DNP-NMR spectroscopy. RSC Advances, 2012, 2, 12812.	3.6	31
61	Impact of Gd ³⁺ on DNP of [1- ¹³ C]Pyruvate Doped with Trityl OX063, BDPA, or 4-Oxo-TEMPO. Journal of Physical Chemistry A, 2012, 116, 5129-5138.	2.5	96
62	Comparison of kinetic models for analysis of pyruvateâ€ŧoâ€ŀactate exchange by hyperpolarized ¹³ C NMR. NMR in Biomedicine, 2012, 25, 1286-1294.	2.8	100
63	Fast Dissolution Dynamic Nuclear Polarization NMR of 13C-Enriched 89Y-DOTA Complex: Experimental and Theoretical Considerations. Applied Magnetic Resonance, 2012, 43, 69-79.	1.2	30
64	DNP by Thermal Mixing under Optimized Conditions Yields >60 000-fold Enhancement of ⁸⁹ Y NMR Signal. Journal of the American Chemical Society, 2011, 133, 8673-8680.	13.7	86
65	Could ¹³ C MRI assist clinical decisionâ€making for patients with heart disease?. NMR in Biomedicine, 2011, 24, 973-979.	2.8	40
66	BDPA: An Efficient Polarizing Agent for Fast Dissolution Dynamic Nuclear Polarization NMR Spectroscopy. Chemistry - A European Journal, 2011, 17, 10825-10827.	3.3	72
67	The effect of ¹³ C enrichment in the glassing matrix on dynamic nuclear polarization of [1- ¹³ C]pyruvate. Physics in Medicine and Biology, 2011, 56, N85-N92.	3.0	36
68	Flux through hepatic pyruvate carboxylase and phosphoenolpyruvate carboxykinase detected by hyperpolarized ¹³ C magnetic resonance. Proceedings of the National Academy of Sciences of the United States of America, 2011, 108, 19084-19089.	7.1	129
69	Competition of pyruvate with physiological substrates for oxidation by the heart: implications for studies with hyperpolarized [1- ¹³ C]pyruvate. American Journal of Physiology - Heart and Circulatory Physiology, 2010, 298, H1556-H1564.	3.2	56
70	Inhibition of carbohydrate oxidation during the first minute of reperfusion after brief ischemia: NMR detection of hyperpolarized ¹³ CO ₂ and H ¹³ CO. Magnetic Resonance in Medicine, 2008, 60, 1029-1036.	3.0	85
71	Hyperpolarized ¹³ C allows a direct measure of flux through a single enzyme-catalyzed step by NMR. Proceedings of the National Academy of Sciences of the United States of America, 2007, 104, 19773-19777.	7.1	266
72	Dipolar cross-relaxation modulates signal amplitudes in the 1H NMR spectrum of hyperpolarized [13C]formate. Journal of Magnetic Resonance, 2007, 189, 280-285.	2.1	26

#	Article	IF	CITATIONS
73	Effects of insulin and cytosolic redox state on glucose production pathways in the isolated perfused mouse liver measured by integrated 2H and 13C NMR. Biochemical Journal, 2006, 394, 465-473.	3.7	35
74	Adiabatic JHSQC for13C isotopomer analysis. Magnetic Resonance in Chemistry, 2006, 44, 463-466.	1.9	4
75	Effect of murine strain on metabolic pathways of glucose production after brief or prolonged fasting. American Journal of Physiology - Endocrinology and Metabolism, 2005, 289, E53-E61.	3.5	57
76	TCA Cycle Turnover And Serum Glucose Sources By Automated Bayesian Analysis Of NMR Spectra. AIP Conference Proceedings, 2004, , .	0.4	0
77	Impaired Tricarboxylic Acid Cycle Activity in Mouse Livers Lacking Cytosolic Phosphoenolpyruvate Carboxykinase. Journal of Biological Chemistry, 2004, 279, 48941-48949.	3.4	141
78	Glucose production, gluconeogenesis, and hepatic tricarboxylic acid cycle fluxes measured by nuclear magnetic resonance analysis of a single glucose derivative. Analytical Biochemistry, 2004, 327, 149-155.	2.4	97
79	Sources of plasma glucose by automated bayesian analysis of2H NMR spectra. Magnetic Resonance in Medicine, 2003, 50, 659-663.	3.0	9
80	Quantifying tracer levels of2H2O enrichment from microliter amounts of plasma and urine by2H NMR. Magnetic Resonance in Medicine, 2001, 45, 156-158.	3.0	53
81	Regulation of Metabolism by Mitochondrial MUL1 E3 Ubiquitin Ligase. Frontiers in Cell and Developmental Biology, 0, 10, .	3.7	2